Generalization of the Use of Random Copolymers To Control the Wetting Behavior of Block Copolymer Films

Shengxiang Ji,[†] Chi-Chun Liu,[†] Jeong Gon Son,[‡] Kevin Gotrik,[§] Gordon S. W. Craig,[†] Padma Gopalan,[||] F. J. Himpsel,[§] Kookheon Char,[‡] and Paul F. Nealey*,[†]

Departments of Chemical and Biological Engineering, Physics, and Materials Science and Engineering, University of Wisconsin, Madison, Wisconsin 53706 and Department of Chemical and Biological Engineering, Seoul National University, Seoul, South Korea 400-004

Received August 14, 2008; Revised Manuscript Received October 6, 2008

ABSTRACT: Random copolymer brushes of poly(styrene-*r*-methyl methacrylate) (PS-*r*-PMMA) have previously been used to control the wetting behavior of poly(styrene-*b*-methyl methacrylate) (PS-*b*-PMMA) block copolymer. Here we demonstrate that the use of random copolymer may be generalized to other block copolymer systems. A series of poly(styrene-*r*-2-vinylpyridine-*r*-hydroxyethyl methacrylate) (PS-*r*-P2VP-*r*-PHEMA) random copolymers was synthesized and evaluated as brush layers to control the orientation of domains in thin films of poly(styrene-*b*-2-vinylpyridine) (PS-*b*-P2VP) block copolymer. On nonpreferential brushes, thin films of PS-*b*-P2VP had a mixed orientation of domains consisting of a perpendicular orientation of lamellar domains near the copolymer−substrate interface and a parallel orientation of lamellar domains at free surface because of the lower surface energy of the PS block. The composition window of brushes that induce vertical orientation of domains near the substrate ranges from 47.8% styrene to 57.0% styrene, as determined by SEM and GISAXS measurements of films after removal of the parallel-oriented domains at surfaces (remaining film thickness ≈ 50 nm). When the PS-*b*-P2VP film was confined between two brushes having compositions within the above range, perpendicular-oriented lamellae that traversed the film thickness were obtained.

Introduction

A perpendicular orientation of domains in block copolymer thin films is desirable for creation of nanoscale templates for pattern transfer applications.[1−5] Several methods, including electric field alignment,[6,7] solvent annealing,[8,9] surfactant-assisted assembly,[10] self-assembly on brush surfaces,[11−20] and directed assembly on chemically patterned surfaces,[13,21−26] have been explored to induce vertical orientation of block copolymer domains in thin films. One of the most promising methods is chemical modification of substrates by random copolymers composed of the same monomers as the block copolymer such that the surfaces are not preferential in wetting behavior toward either block of the copolymer.[16−20] The seminal work of Mansky et al. showed that grafting an end hydroxyl poly(styrene-*r*-methyl methacrylate) (PS-*r*-PMMA) random copolymer to a silicon substrate could elicit the perpendicular domain formation in poly(styrene-*b*-methyl methacrylate) (PS-*b*-PMMA) thin films.[16] As the styrene fraction in the PS-*r*-PMMA coating was increased from 0 to 1, the substrate transitioned from PMMA wetting to PS wetting, and they reported the optimal condition for perpendicular orientation of domains occurring at a styrene fraction of 0.58. More recent research by Ryu et al.,[17] In et al.,[18] Han et al.,[19] and Bang et al.[20] demonstrated that incorporation of a few percentage of a third monomer, e.g., benzocyclobutene, hydroxyethyl methacrylate (HEMA), epoxy, acrylate, and azide groups, into PS-*r*-PMMA allowed them to deposit brushes on substrates through either cross-linking or covalently bonding to control the orientation of PS-*b*-PMMA domains.

The vast majority of research has focused on thin films of PS-*b*-PMMA. One attractive property of this system with respect to formation of perpendicular structures is that the surface energy difference of PS and PMMA is close to zero at convenient annealing temperatures and a perpendicular orientation of domains throughout the film can be achieved on nonpreferential substrates.[27] For most block copolymers other than PS-*b*-PMMA a large surface energy difference between blocks can result in preferential wetting of one block at the free surface of the film and lead to a parallel orientation of domains.[27] Few studies on other copolymers have been reported, probably at least in part due to the need to control both the surface energy difference between blocks and the interfacial energy difference between each block and the substrate to achieve vertically oriented domains that propagate entirely through the film thickness. Alternatively, nonequilibrium processing such as solvent annealing can be used to achieve vertical orientation of copolymers that have a large surface energy difference between their respective blocks, such as poly(styrene-*b*-2-vinylpyridine-*b*-*tert*-butyl methacrylate) (PS-*b*-P2VP-*b*-P^{t}BA),[28] poly(isoprene-*b*-lactide) (PI-*b*-PLA),[29] and poly(styrene-*b*-ethylene oxide) (PS-*b*-PEO).[8]

Here we explore the use of PS-*r*-P2VP random copolymers to modify the substrates to control the domain orientation in PS-*b*-P2VP films. Our rational for choosing PS-*b*-P2VP in this work is that its blocks exhibit a large difference in surface energy, which makes PS-*b*-P2VP a representative model system for block copolymers with large surface energy differences.[27] Additionally, PS-*b*-P2VP has been widely studied for both scientific and technological purposes.[30−34] It has many potential applications, such as the selective incorporation of functional moieties into the P2VP block that are electrically or optically active[35−37] or enhancement of etch selectivity in pattern transfer operations.[38,39] Following In et al.,[18] the mechanism of random copolymer attachment to the substrate that we used involved incorporation of ∼2 mol % hydroxyl groups in the random copolymer. The resulting random copolymer, poly(styrene-*r*-2-vinylpyridine-*r*-hydroxyethyl methacrylate) (PS-*r*-P2VP-*r*-PHEMA), was designed to provide a brush surface for PS-*b*-

* To whom correspondence should be addressed. E-mail: nealey@engr.wisc.edu.
[†] Department of Chemical and Biological Engineering, University of Wisconsin.
[‡] Seoul National University.
[§] Department of Physics, University of Wisconsin.
[||] Department of Materials Science and Engineering, University of Wisconsin.

10.1021/ma801861h CCC: $40.75
Published on Web 11/11/2008

Scheme 1. Synthesis of PS-*r*-P2VP-*r*-PHEMA Random Copolymer

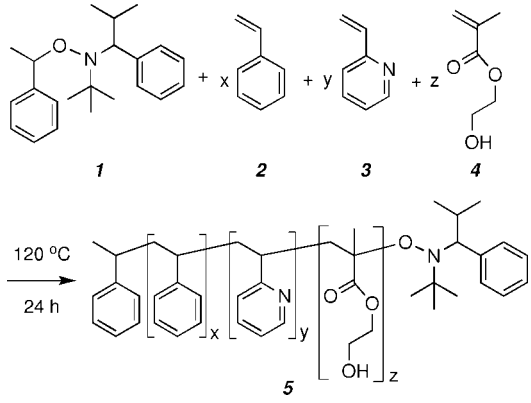

P2VP via subsequent covalent bonding of the hydroxyl groups in the HEMA monomer to the silicon substrate.

Experimental Section

A. Materials. Styrene (S, **2**), 2-vinylpyridine (2VP, **3**), and hydroxyethyl methacrylate (HEMA, **4**) were purchased from Aldrich and purified through an Al_2O_3 column before use. PS-*b*-P2VP (M_n = 52−57 kg/mol (52−57K), natural period $L_o \approx 69$ nm, PDI = 1.08; 40−40 kg/mol (40−40K), $L_o \approx 53$ nm, PDI = 1.07) and PS-*b*-PMMA (M_n = 52−52 kg/mol (52−52K), $L_o \approx 49$ nm, PDI = 1.05) were purchased from Polymer Source, Inc. The alkoxyamine initiator, 2,2,5-trimethyl-3-(1-phenylethoxy)-4-phenyl-3-azahexane, was synthesized as reported in the literature.[40] Tetrahydrofuran (THF), *N*,*N*-dimethylformamide (DMF), and hexanes were purchased from Aldrich and used as received.

B. Polymerization of PS-*r*-P2VP-*r*-PHEMA (5) and Thin Film Preparation. Random copolymers (**5** in Scheme 1) were synthesized with 2 mol % of HEMA and varying compositions of S and 2VP by nitroxide-mediated controlled radical polymerization (NMP).[18] A representative polymerization procedure is described for the synthesis of copolymer 51.5S. A mixture of initiator **1** (0.0244 g, 0.075 mmol), S (1.155 g, 11.1 mmol), 2VP (0.903 g, 8.6 mmol), and HEMA (0.042 g, 0.32 mmol) was degassed by three freeze−thaw cycles. The mixture was heated at 120 °C for 24 h under a nitrogen atmosphere. Conversion of both S and 2VP in the random copolymerization was determined to be greater than 95% in all cases. The resulting copolymers were dissolved in THF and then precipitated in hexanes. The fraction of S in final copolymers was determined by ^{1}H NMR spectroscopy.

Thin films of PS-*r*-P2VP-*r*-PHEMA were deposited on piranha-cleaned silicon wafers by spin coating at 4000 rpm from a 1 wt % DMF solution. The samples were then annealed at 160 °C for 24 h to create a covalent bond between PS-*r*-P2VP-*r*-PHEMA and the silicon substrate as before.[18] Unbound polymers were removed by repeated sonication in warm DMF. Solutions of PS-*b*-P2VP in DMF were then spin coated on PS-*r*-P2VP-*r*-PHEMA-coated silicon wafers and annealed at 170 °C for 3 days under vacuum to develop the equilibrium morphology. The sandwiched structure was prepared by spin coating the copolymer solution on a PS-*r*-P2VP-*r*-PHEMA-modified substrate. Another PS-*r*-P2VP-*r*-PHEMA-modified substrate was placed on the film surface and clamped in place. After annealing and cooling to room temperature, the top cover was removed by inserting a razor blade between the two wafers. Analysis was performed on areas where fracture occurred at the interface between the polymer film and the top surface.

C. Instrumentation. ^{1}H NMR spectra were recorded on a Varian UNITY 500 spectrometer. M_n and polydispersity index (PDI) of the copolymers were determined by gel permeation chromatography (GPC) relative to a PS standard with THF as the eluent. Film thicknesses were measured with a Rudolph ellipsometer. The static contact angle of deionized water was measured at ambient temperature using a Future Digital Scientific model OCA15 video goniometer. A LEO 1550 VP field-emission scanning electron microscope (SEM) was used to image the block copolymer films using a 1 kV acceleration voltage. To increase the contrast between the PS and the P2VP domains in the SEM images, SEM samples were exposed to saturated I_2 vapor in a sealed glass gar for 6−8 h, which selectively stained the P2VP domains. The surface topography of the thin films was imaged using a NanoScope IIIa multimode atomic force microscope (AFM, Digital Instruments) with an ultrasharp cantilever tip (NSC15/no Al, MikroMasch Inc.) in tapping mode. Small angle X-ray scattering (SAXS) measurements were performed on a Ragaku SAXS system at the Materials Science Center, University of Wisconsin. The sample was annealed at 190 °C under vacuum for 30 min before measurement. Oxygen plasma treatment was performed on a Uniaxis 790 RIE etcher (Plasma-Therm, Inc.) at the Wisconsin Center for Advanced Microelectronic (WCAM) at the University of Wisconsin. For the purpose of removing surface layers of the block copolymer film, the oxygen plasma was operated at 35 °C, 50 W power, 10 mTorr pressure, and an oxygen flow rate of 10 SCCM. Because PS and P2VP have similar etch selectivity under our optimized conditions, plasma etching did not induce significant surface roughness.

Near edge X-ray atomic fine structure (NEXAFS) measurements were performed at the Synchrotron Radiation Center (SRC) of the University of Wisconsin. Absorption spectra of the brushes were taken at the C 1s edge in the total electron yield mode. The stoichiometry was determined by fitting the data with an interpolation between three normalized reference spectra (from the homopolymers PS and P2VP and from the 50/50 wt % diblock copolymer PS-*b*-P2VP). The data reported here were collected at normal incidence. They were independent of the incidence angle.

Grazing incidence small angle X-ray scattering (GISAXS) measurements were performed at Beamline 4C2 at the Pohang Synchrotron Radiation Center, South Korea, with a wavelength of $\lambda = 1.3807$ Å. We used 40−40K PS-*b*-P2VP ($L_o \approx 53$ nm) instead of 52−57K PS-*b*-P2VP ($L_o \approx 69$ nm) for GISAXS analysis because the lower M_n copolymer will have a peak at a higher q value, and therefore, the GISAXS peak was not blocked by the beam stop present at low q. GISAXS patterns of each sample were taken at an incidence angle ranging from 0.10° to 0.20°, which spanned the critical angle for the copolymer samples ($\alpha_C \approx 0.14-15°$) and was below the silicon critical angle.

Results and Discussion

The PS-*r*-P2VP-*r*-PHEMA random copolymer was successfully synthesized by NMP. The styrene (S) contents in feed, bulk polymers, and their corresponding brushes are summarized in Table 1. The percentage of S units in the final, purified copolymers was 2.4−5.4% lower than the percentage of S in feed, by ^{1}H NMR analysis. On the basis of the reactivity ratio of S and 2VP ($r_{2VP,S} = 1.26$ and $r_{S,2VP} = 0.53$) we could estimate that the random copolymers would be P2VP enriched at the early stages of copolymerization and PS enriched at the later stages.[41] The M_n values of all 11 PS-*r*-P2VP-*r*-PHEMA samples were ∼30 000 g/mol with PDI of ∼1.25. The average number of hydroxyl groups per chain was estimated to be ∼4 based on 2 mol % HEMA in the copolymerization reactants.

After deposition the brushes were characterized by ellipsometry, AFM, goniometry, and NEXAFS to determine the thickness, surface topography, contact angles, and chemical compositions, respectively. The film thickness of the PS-*r*-P2VP-*r*-PHEMA was measured to be ∼5−6 nm, similar to previous work with PS-*r*-PMMA-*r*-PHEMA brushes.[18] No phase contrast or topographical difference was observed in AFM analysis of the brushes. Static contact angles of water on the brush layers increased monotonically with increasing styrene content in the random copolymers and were between the measured contact angles of pure PS (92.8°) and pure P2VP (61.7°) (Table 1). The brush composition could be different from the bulk composition of the random copolymer due to the nature of the

Table 1. Characteristics of PS-*r*-P2VP-*r*-PHEMA (5) Copolymer Brushes

	sample[a]										
	25.9S	35.6S	41.8S	42.5S	44.6S	47.8S	51.5S	52.4S	57.0S	60.8S	67.6S
%S in feed	30.0	40.0	45.0	47.5	50.0	52.5	55.0	57.5	60.0	65.0	70.0
%S found[b]	25.9	35.6	41.8	42.5	44.6	47.8	51.5	52.4	57.0	60.8	67.6
%S found[c]	34 ± 5	37 ± 2	43 ± 4	45 ± 2	47 ± 4	50 ± 2	52 ± 3	54 ± 3	57 ± 4	63 ± 3	68 ± 3
contact angle[d]	70	72	74	75	76	77	77	77	78	79	79

[a] 44.6S represents that the mol % S found in the copolymer was 44.6 mol %. It also has 2 mol % HEMA and 53.4 mol % 2VP. [b] By ^{1}H NMR spectroscopy. [c] By NEXAFS. [d] Static water contact angle; 2% error based on three measurements. Water contact angles of PS and P2VP were 92.8° and 61.7°, respectively.

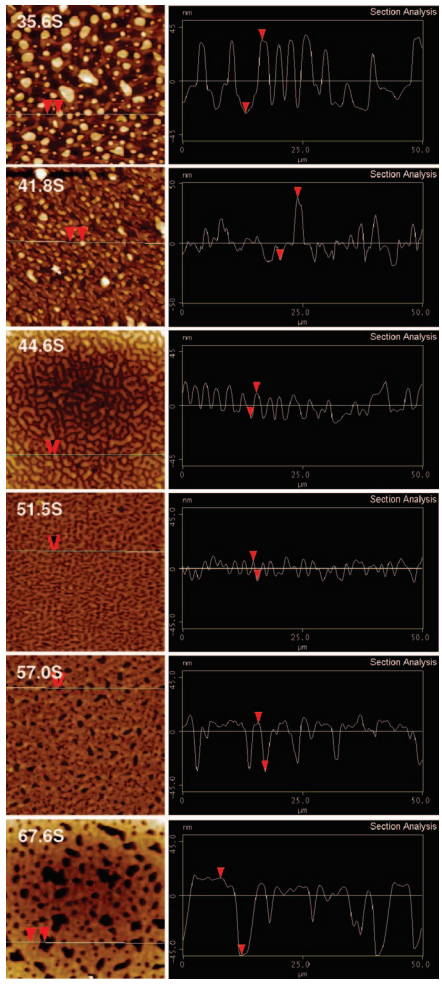

Figure 1. AFM of 52−57K PS-*b*-P2VP (L_o = 69 nm) annealed at 170 °C for 3 days on PS-*r*-P2VP-*r*-PHEMA brushes of varying styrene content: (left column) height images of 50 μm × 50 μm sections; (right column) topographical analysis. Initial film thickness: $t_o \approx$ 130 nm (~1.9 L_o). An island-to-hole transition was observed as the brush composition progressed from 35.6S to 67.6S.

random copolymerization. To correlate the compositions in bulk and on brushes NEXAFS was used to probe the composition in the thin brush layers.[15,42] The representative NEXAFS spectra are shown in Figure S1 of the Supporting Information. Insertion of a nitrogen (N) atom into the aromatic carbon (C) ring of P2VP creates a distinct additional peak in the π^* region. It originates from the two C atoms adjacent to the N whose C 1s level is shifted toward higher binding energy due to charge transfer to the N. The stoichiometry of S and 2VP was determined by fitting the data with an interpolation between three normalized reference spectra. The brush compositions determined by NEXAFS agreed well with their corresponding bulk compositions from ^{1}H NMR analysis (Table 1). We quote the bulk compositions as the final compositions of the brushes for this paper.

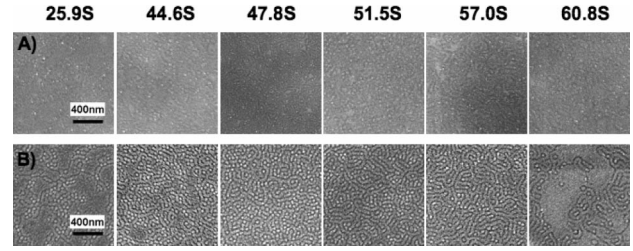

Figure 2. Difference in domain orientation with film thickness, as shown by SEM images of PS-*b*-P2VP (40−40K) films on substrates treated with random copolymers after oxygen plasma etching (with I_2 staining): (A and B) the remaining film thicknesses were ~50 and ~30 nm, respectively.

The brush compositions that induce perpendicular orientation of domains near the substrate were determined by AFM measurement of the film topography. Previous research has shown that the preferential wetting behavior of PS or P2VP to the substrate will produce hole or island structures when the film thickness deviates from the characteristic values of $(n + 1/2)L_o$ for asymmetric wetting and nL_o for symmetric wetting, where n represents quanta of the bulk lamellar period L_o.[43−45] We analyzed the morphology of 130 nm thick films of PS-*b*-P2VP (52−57K, $L_o \approx$ 69 nm). For a lamellae-forming block copolymer with a film thickness of 1.9 L_o, as is the case here, holes will form when one of the blocks resides at both the interface and the free surface of the film (symmetric wetting) and islands will form when one block resides at the interface and the other block resides at the free surface (asymmetric wetting). Figure 1 shows the tapping-mode height images of six representative films and their corresponding sectional analyses. PS-*b*-P2VP showed different preferential wetting behaviors on PS-rich and P2VP-rich substrates. For example, island formation was observed for 35.6S- and 41.8S-modified substrates, which indicated asymmetric wetting with the P2VP block at the substrates. At the other end of the spectrum of brush compositions, PS-*b*-P2VP on the 57.0S- and 67.6S-modified substrates formed holes with the PS block at the substrates. The island (35.6S and 41.8S, asymmetric wetting) to hole (57.0S and 67.6S, symmetric wetting) transition was clearly observed when we changed the compositions of PS-*r*-P2VP-*r*-PHEMA copolymer brushes from 35.6S to 67.6S. The composition for nonpreferential wetting toward both blocks should occur in the vicinity of the island-to-hole transition point for a noncommensurate film thickness.[10] Topographical analysis showed that the roughness decreased with increasing S up to 51.5 mol % S and then increased as the S content increased beyond 51.5 mol %. The root-mean-square roughness (R_q) values of the six samples on PS-*r*-P2VP-*r*-PHEMA-modified substrates (from 35.6S to 67.6S) were 17.4, 16.9, 11.5, 5.8, 8.3, and 18.3 nm. 51.5S had the smallest R_q compared to the other five samples, suggesting that the composition for nonpreferential wetting should be close to 51.5S. Similar analyses of the hole/island transition were used by Peters et al. to identify the nonpreferential wetting composition for PS-*b*-PMMA on SAMs.[10] In their work PS-*b*-PMMA

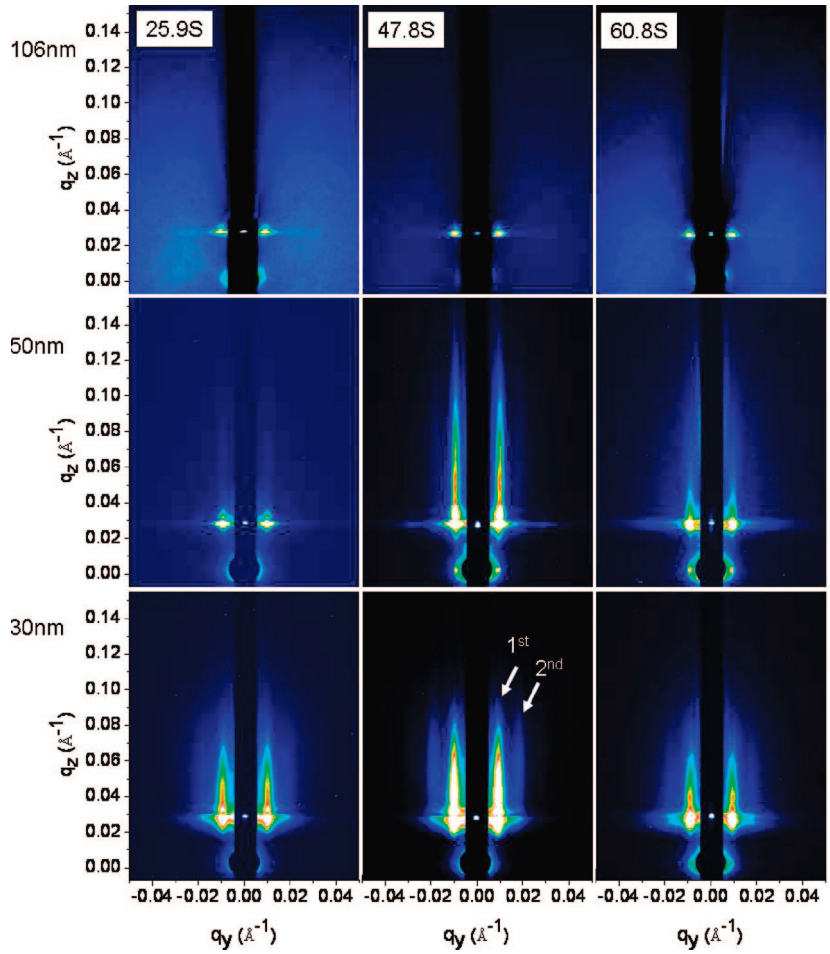

Figure 3. Difference in domain orientation with film thickness, as shown by GISAXS of three different thicknesses of 40−40K PS-*b*-P2VP films on three representative PS-*r*-P2VP-modified substrates. The arrows indicated the first- and second-order peaks attributed to the lamellar structure. GISAXS was performed with an incidence angle of 0.16°. The two thinner sets of films were generated from an oxygen etch back of the 106 nm thick film.

film was featureless on a specific SAM, which was characteristic of nonpreferential wetting behavior.

More convincing evidence of some of the random copolymer brushes inducing perpendicular orientation near the substrate came from SEM and GISAXS analysis of PS-*b*-P2VP films that were partially etched by oxygen plasma to expose the domain structure within the film. The initial film thickness was 106 nm ($\sim 2L_o$, $L_o \approx 53$ nm for $M_n = 40-40$K PS-*b*-P2VP). We did not observe perpendicular lamellae at the free surface with SEM because the PS block had a lower surface energy and therefore resided at the free surface of the film. In order to probe the film structures near the substrate region an oxygen plasma etching process was used to remove the top surface layers of the films. After removal of ~56 nm of the film at the surface (the remaining film thickness was ~50 nm), the onset of fingerprint-like structures was present in the assembled films on brushes 47.8S, 51.5S, and 57.0S (Figure 2A). A clearer picture of fingerprint-like structures in the films that were etched to a thickness of 30 nm confirmed that the perpendicular structure was formed near the substrate interface in Figure 2B. We observed the change in domain orientation with the increase of styrene fraction in the brushes from a mixed (perpendicular and parallel) lamellar orientation on brushes 25.9S and 44.6S to a perpendicular orientation on brushes 47.8S, 51.5S, and 57.0S to a mixed orientation on brush 60.8S. The exact origin of the white dots in SEM mages is unknown, but they could be iodine aggregates or the dotted domains due to damage from RIE. The styrene content (47.8S−57.0S) in the brushes for a perpendicular orientation of PS-*b*-P2VP domains was similar to that in random copolymer brushes found to be chemically neutral for PS-*b*-PMMA (~58% styrene).[16,18]

GISAXS, a nondestructive technique to probe the average three-dimensional orientation of domains over large areas, was used to probe the film structures on the 11 brushes in this study. The GISAXS patterns ($\alpha = 0.16°$) of films on three representative brushes (25.9S, 47.8S, and 60.8S) before and after oxygen plasma etching are shown in Figure 3. For films with a thickness of 106 nm, the intensity of first-order peaks was very low due to the presence of parallel oriented domains on the free surface of the films.[46] After removal of ~56 nm of the films (remaining thickness ≈ 50 nm) a strong scattering peak at $q_y = 0.0118$ Å^{-1} appeared from the film deposited on 47.8S brush, corresponding to a perpendicular orientation of lamellar domains in the film with a d spacing of 53.4 nm, which agrees with the bulk natural lamellar period ($L_o = 53.2$ nm) of 40−40K PS-*b*-P2VP, as determined by SAXS. Comparing GISAXS profiles of 50 nm thick PS-*b*-P2VP films on all 11 brushes that we tested (Figure 4) we found that the scattering intensity increased with the increase of styrene content from brush 25.9S to brush 47.8S, and then the scattering intensity dropped as the styrene content was increased beyond 47.8S. After removal of an additional 20 nm of film (remaining thickness ≈ 30 nm) a second-order peak with $q = 0.0235$ Å^{-1} appeared on brush 47.8S (Figure 3), which correlated to the presence of perpendicular lamellar domains in the SEM image, as shown in Figure 2B.[47] The appearance of the more-intense first-order scattering peak in films on brushes 25.9S and 60.8S also indicated the presence of a portion of perpendicular domains near the substrate interface on these two

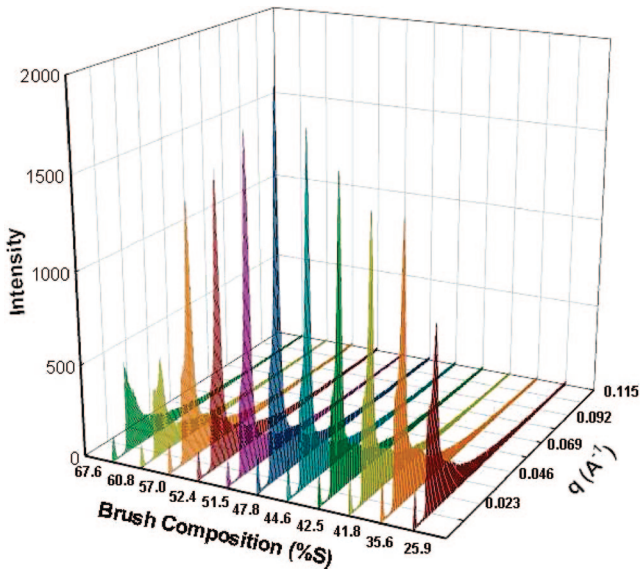

Figure 4. 3D plot of 2D GISAXS profiles of 50 nm thick PS-*b*-P2VP (40K−40K) films on 11 brushes at $\alpha = 0.16°$. The scattering intensity increased with the increase of styrene content from brush 25.9S to brush 47.8S, indicative of increased uniformity of domain orientation, and then dropped as with styrene content was increased beyond 47.8S.

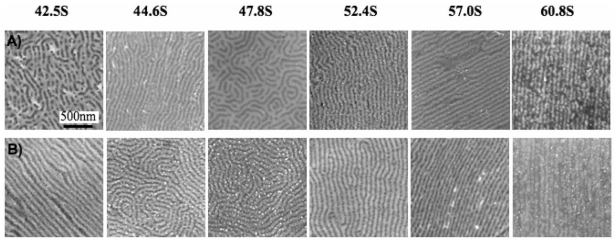

Figure 5. Top-down SEM images of perpendicular domains at the top surface of 40−40K PS-*b*-P2VP films sandwiched between two substrates modified with PS-*r*-P2VP-*r*-PHEMA brushes (after I_2 staining): (A) film thickness ≈ 47 nm (0.7 L_o); (B) film thickness ≈ 105 nm (1.5 L_o). White particles or spots in the SEM image could be from iodine aggregates or silicon oxide particles from the substrates.

brushes, which is consistent with the fact that there were more perpendicular domains observed in the etched films by SEM analysis in Figure 2B.

We could construct a schematic of the internal domain structure of PS-*b*-P2VP films throughout the film thickness based on both SEM and GISAXS analysis.[20,48] The domain structure consisted of a mixed morphology of perpendicular lamellar domains that propagate ∼50 nm from the substrate interface but transition to parallel lamellae at the air interface due to the affinity of the PS block for the free surface of the film. In another study by Wang et al. Monte Carlo simulation of copolymers confined between neutral and strong preferential boundary conditions supported the presence of the described mixed morphology that we observed experimentally.[49]

To assemble perpendicular structures throughout the film thickness a series of 47 nm thick (∼0.7 L_o) and 105 nm thick (∼1.5 L_o) films of 40−40K PS-*b*-P2VP were sandwiched and annealed between two PS-*r*-P2VP-*r*-PHEMA-treated substrates. Perpendicular alignment of PS-*b*-P2VP domains at the substrate interface was evidenced by the top-down SEM analysis of the films after removing one of the brush-coated substrates.[15] Among these modified substrates, brushes 44.6S, 47.8S, 51.5S, and 52.4S induced vertical alignment of PS-*b*-P2VP domains for both of thicknesses that were tested, and representative SEM images are shown in Figure 5. The other PS-*r*-P2VP-*r*-PHEMA-treated substrates, e.g., 42.5S, 57.0S, and 60.8S, induced PS-*b*-P2VP morphologies with either disconnections or missing domains due to the deviations of S and 2VP fractions from the composition window for vertical orientation of PS-*b*-P2VP domains (Figure 5). Kellog et al.[50] studied two different confinement conditions, e.g., PS-*r*-PMMA-covered nonpreferential walls and preferential walls, for PS-*b*-PMMA films. They also found that perpendicular orientation of domains of PS-*b*-PMMA throughout the film thickness was only achieved under confinement of PS-*r*-PMMA-covered nonpreferential walls. The composition window ($44.6 < \%S < 57.0$) for perpendicular orientation of domains confined between two brushes was similar to the window determined from both SEM and GISAXS measurements. In most cases, the patterns were aligned in one direction, which may have been caused by shear during clamping.[15,51] Similar alignment effects were also observed for 52K−52K PS-*b*-PMMA films with a thickness of 1.0 L_o and 1.5 L_o sandwiched between two PS-*r*-PMMA (58%S) modified substrates (see Supporting Information, Figure S2).

Conclusion

This work demonstrated the generalizablility of using random copolymer brushes as a nonpreferential surface for assembly of block copolymers with large surface energy differences, such as PS-*b*-P2VP. Brushes within a composition range from 47.8S to 57.0S induced vertical orientation of domains near the brush-modified substrate in PS-*b*-P2VP thin films, which was evidenced from both the analysis of island−hole configurations seen in AFM and the SEM images and GISAXS measurements of oxygen plasma-etched PS-*b*-P2VP films on brush surfaces. The fact that the method presented here created nonpreferential surfaces as well as vertically oriented lamellae for block copolymers with blocks that have very different surface energies provides further evidence that the method should be applicable to a broad variety of block copolymers as long as it is feasible to synthesize the corresponding random copolymer.

Acknowledgment. The authors thank the UW-NSF Nanoscale Science and Engineering Center (NSEC) (DMR 0425880) and the center on Functional Engineered Nano Architectonics (FENA) at UCLA for financial support. The NEXAFS work was performed at the SRC, which is supported by NSF DMR-0537588.

Supporting Information Available: NEXAFS profiles of PS-*b*-P2VP, homopolymers PS and P2VP, brush 44.6S, and the fitted curve; SEM images of 52−52K PS-*b*-PMMA films sandwiched between PS-*r*-PMMA modified substrates. This material is available free of charge via the Internet at http://pubs.acs.org.

References and Notes

(1) Black, C. T.; Guarini, K. W.; Milkove, K. R.; Baker, S. M.; Russell, T. P.; Tuominen, M. T. *Appl. Phys. Lett.* **2001**, *79*, 409–411.
(2) Black, C. T. *Appl. Phys. Lett.* **2005**, *87*, 163116.
(3) Guarini, K. W.; Black, C. T.; Milkove, K. R.; Sandstrom, R. L. *J. Vac. Sci. Technol. B* **2001**, *19*, 2784–2788.
(4) Cheng, J. Y.; Ross, C. A.; Chan, V. Z. H.; Thomas, E. L.; Lammertink, R. G. H.; Vancso, G. J. *Adv. Mater.* **2001**, *13*, 1174–1178.
(5) Park, M.; Harrison, C.; Chaikin, P. M.; Register, R. A.; Adamson, D. H. *Science* **1997**, *276*, 1401–1404.
(6) Amundson, K.; Helfand, E.; Davis, D. D.; Quan, X.; Patel, S. S.; Smith, S. D. *Macromolecules* **1991**, *24*, 6546–6548.
(7) Morkved, T. L.; Lu, M.; Urbas, A. M.; Ehrichs, E. E.; Jaeger, H. M.; Mansky, P.; Russell, T. P. *Science* **1996**, *273*, 931–933.
(8) Kim, S. H.; Misner, M. J.; Russell, T. P. *Adv. Mater.* **2004**, *16*, 2119–2123.
(9) Kim, S. H.; Misner, M. J.; Xu, T.; Kimura, M.; Russell, T. P. *Adv. Mater.* **2004**, *16*, 226–231.
(10) Son, J. G.; Bulliard, X.; Kang, H.; Nealey, P. F.; Char, K. *Adv. Mater.* **2008**, *20*, 3643–3648.
(11) Peters, R. D.; Yang, X. M.; Kim, T. K.; Sohn, B. H.; Nealey, P. F. *Langmuir* **2000**, *24*, 4625–4631.

(12) Peters, R. D.; Yang, X. M.; Wang, Q.; de Pablo, J. J.; Nealey, P. F. *J. Vac. Sci. Technol. B* **2000**, *18*, 3530–3534.
(13) Kim, S. O.; Solak, H. H.; Stoykovich, M. P.; Ferrier, N. J.; de Pablo, J. J.; Nealey, P. F. *Nature* **2003**, *424*, 411–414.
(14) Peters, R. D.; Yang, X. M.; Kim, T. K.; Nealey, P. F. *Langmuir* **2000**, *24*, 9620–9626.
(15) Ji, S.; Liu, G.; Zheng, F.; Craig, G. S. W.; Himpsel, F. J.; Nealey, P. F. *Adv. Mater.* **2008**, *20*, 3054–3060.
(16) Mansky, P.; Liu, Y.; Huang, E.; Russell, T. P.; Hawker, C. *Science* **1997**, *275*, 1458–1460.
(17) Ryu, D. Y.; Shin, K.; Drockenmuller, E.; Hawker, C. J.; Russell, T. P. *Science* **2005**, *308*, 236–239.
(18) In, I.; La, Y. H.; Park, S. M.; Nealey, P. F.; Gopalan, P. *Langmuir* **2006**, *22*, 7855–7860.
(19) Han, E.; In, I.; La, Y.; Park, S.; Wang, Y.; Nealey, P. F.; Gopalan, P. *Adv. Mater.* **2007**, *19*, 4448–4452.
(20) Bang, J.; Bae, J.; Löwenhielm, P.; Spiessberger, C.; Given-Beck, S. A.; Russell, T. P.; Hawker, C. J. *Adv. Mater.* **2007**, *19*, 4552–4557.
(21) Edwards, E. W.; Montague, M. F.; Solak, H. H.; Hawker, C. J.; Nealey, P. F. *Adv. Mater.* **2004**, *16*, 1315–1319.
(22) Edwards, E. W.; Muller, M.; Stoykovich, M. P.; Solak, H. H.; de Pablo, J. J.; Nealey, P. F. *Macromolecules* **2007**, *40*, 90–96.
(23) La, Y. H.; Edwards, E. W.; Park, S. M.; Nealey, P. F. *Nano Lett.* **2005**, *5*, 1379–1384.
(24) Stoykovich, M. P.; Edwards, E. W.; Solak, H. H.; Nealey, P. F. *Phys. Rev. Lett.* **2006**, *97*, 147802.
(25) Stoykovich, M. P.; Muller, M.; Kim, S. O.; Solak, H. H.; Edwards, E. W.; de Pablo, J. J.; Nealey, P. F. *Science* **2005**, *308*, 1442–1446.
(26) Park, S. M.; Craig, G. S. W.; La, Y. H.; Solak, H. H.; Nealey, P. F. *Macromolecules* **2007**, *40*, 5084–5094.
(27) Sauer, B. B.; Dee, G. T. *Macromolecules* **2002**, *35*, 7024–7030.
(28) Ludwigs, S.; Schmidt, K.; Stafford, C. M.; Amis, E. J.; Fasolka, M. J.; Karim, A.; Magerle, R.; Krausch, G. *Macromolecules* **2005**, *38*, 1850–1858.
(29) Cavicchi, K. A.; Russell, T. P. *Macromolecules* **2007**, *40*, 1181–1186.
(30) Heier, J.; Genzer, J.; Kramer, E. J.; Bates, F. S.; Walheim, S.; Krausch, G. *J. Chem. Phys.* **1999**, *111*, 11101–11110.
(31) Chiu, J. J.; Kim, B. J.; Kramer, E. J.; Pine, D. J. *J. Am. Chem. Soc.* **2005**, *127*, 5036–5037.
(32) Abes, J. I.; Cohen, R. E.; Ross, C. A. *Chem. Mater.* **2003**, *15*, 1125–1131.
(33) Li, X.; Peng, J.; Wen, Y.; Kim, D. H.; Knoll, W. *Polymer* **2007**, *48*, 2434–2443.
(34) Yokoyama, H.; Mates, T. E.; Kramer, E. J. *Macromolecules* **2000**, *33*, 1888–1898.
(35) Laforgue, A.; Bazuin, C. G.; Prud'homme, R. E. *Macromolecules* **2006**, *39*, 6473–6482.
(36) Sidorenko, A.; Tokarev, I.; Minko, S.; Stamm, M. *J. Am. Chem. Soc.* **2003**, *125*, 12211–12216.
(37) Valkama, S.; Ruotsalainen, T.; Nykanen, A.; Laiho, A.; Kosonen, H.; ten Brinke, G.; Ikkala, O.; Ruokolainen, J. *Macromolecules* **2006**, *39*, 9327–9336.
(38) Chai, J.; Wang, D.; Fan, X. N.; Buriak, J. M. *Nat. Nanotechnol.* **2007**, *2*, 500–506.
(39) Haupt, M.; Miller, S.; Glass, R.; Arnold, M.; Sauer, R.; Thonke, K.; Moller, M.; Spatz, J. P. *Adv. Mater.* **2003**, *15*, 829–831.
(40) Benoit, D.; Chaplinski, V.; Braslau, R.; Hawker, C. J. *J. Am. Chem. Soc.* **1999**, *121*, 3904–3920.
(41) Odian, G. *Principles of Polymerization*; John Wiley & Sons, Inc.: **New York**, **2004**.
(42) Ade, H.; Hitchcock, A. P. *Polymer* **2008**, *49*, 643–675.
(43) Coulon, G.; Collin, B.; Ausserre, D.; Chatenay, D.; Russell, T. P. *J. Phys.* **1990**, *51*, 2801–2811.
(44) Smith, A. P.; Douglas, J. F.; Meredith, J. C.; Amis, E. J.; Karim, A. *Phys. Rev. Lett.* **2001**, *87*, 015503.
(45) Heier, J.; Kramer, E. J.; Groenewold, J.; Fredrickson, G. H. *Macromolecules* **2000**, *33*, 6060–6067.
(46) Busch, P.; Posselt, D.; Smilgies, D.-M.; Rauscher, M.; Papadakis, C. M. *Macromolecules* **2007**, *40*, 630–640.
(47) Khanna, V.; Cochran, E. W.; Hexemer, A.; Stein, G. E.; Fredrickson, G. H.; Kramer, E. J.; Li, X.; Wang, J.; Hahn, S. F. *Macromolecules* **2006**, *39*, 9346–9356.
(48) Huang, E.; Rockford, L.; Russell, T. P.; Hawker, C. J. *Nature* **1998**, *395*, 757–758.
(49) Wang, Q.; Yan, Q. L.; Nealey, P. F.; de Pablo, J. J. *J. Chem. Phys.* **2000**, *112*, 450–464.
(50) Kellog, G. J.; Walton, D. G.; Mayes, A. M.; Lambooy, P.; Russell, T. P.; Gallagher, P. D.; Satija, S. K. *Phys. Rev. Lett.* **1996**, *76*, 2503–2506.
(51) Register, R. A.; Angelescu, D. E.; Pelletier, V.; Asakawa, K.; Wu, M. W.; Adamson, D. H.; Chaikin, P. M. *J. Photopolym. Sci. Technol.* **2007**, *20*, 493–498.

MA801861H